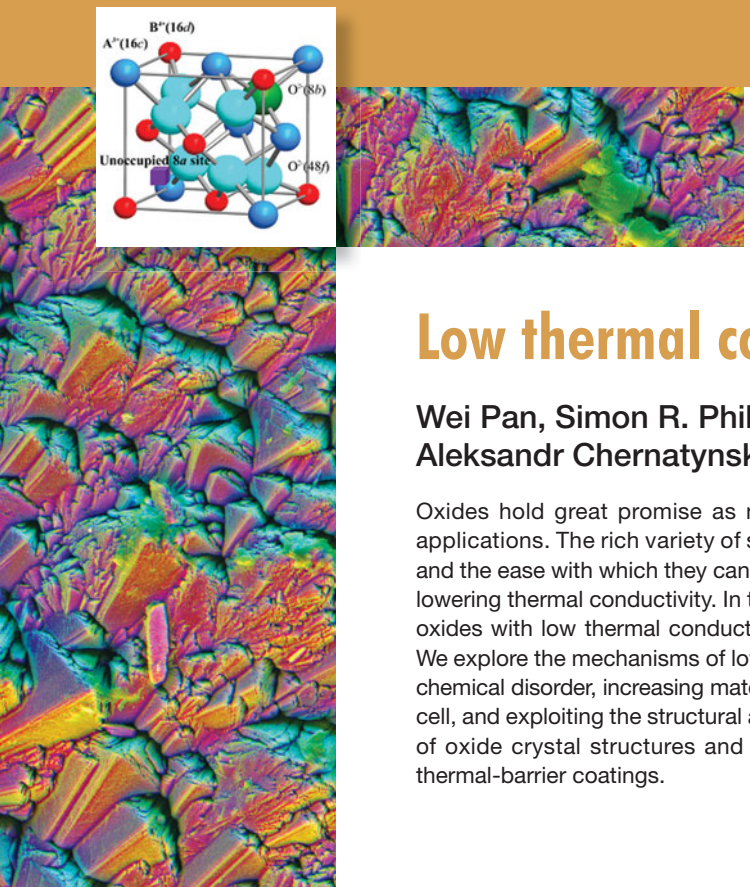


Low thermal conductivity oxides

Wei Pan, Simon R. Phillpot, Chunlei Wan, Aleksandr Chernatynskiy, and Zhixue Qu

Oxides hold great promise as new and improved materials for thermal-barrier coating applications. The rich variety of structures and compositions of the materials in this class, and the ease with which they can be doped, allow the exploration of various mechanisms for lowering thermal conductivity. In this article, we review recent progress in identifying specific oxides with low thermal conductivity from both theoretical and experimental perspectives. We explore the mechanisms of lowering thermal conductivity, such as introducing structural/chemical disorder, increasing material density, increasing the number of atoms in the primitive cell, and exploiting the structural anisotropy. We conclude that further systematic exploration of oxide crystal structures and chemistries are likely to result in even further improved thermal-barrier coatings.

Introduction

The need for thermal-barrier coating (TBC) materials with lower thermal conductivity than the currently used 7% yttria-stabilized zirconia (7YSZ) composition that can also operate in the strongly oxidative environment of combustion gases has stimulated a worldwide effort to identify new oxide compositions (see the introductory article in this issue). It has also stimulated a better understanding of the factors that determine low thermal conductivity in crystalline solids at high temperatures. Although TBC materials must satisfy a wide range of requirements, the primary performance metric is their thermal conductivity at operating temperatures of 1250°C and above. Depending on the processing technology and conditions, the thermal conductivity of 7YSZ lies in the range of 1.2–1.8 W m^{-1} K^{-1}; we are therefore most interested in materials with thermal conductivities below ~1 W m^{-1} K^{-1}. For the foreseeable future, the operating temperatures are still not high enough for appreciable radiative heat transfer unless the coating material contains ions that absorb in the infrared.[1] As this article will describe, an impressive number of new oxide materials have been identified in the last decade that have conductivities lower than 7YSZ; the thermal conductivities of the emerging ceramics for TBC are summarized in **Figure 1**a–b. There are good reasons to believe that the continued search, combining crystal chemistry principles and simulation, will identify others. Unless otherwise noted, all the conductivity values presented are for fully dense materials without porosity, since porosity can significantly reduce the measured conductivity. Indeed, porosity is deliberately introduced into TBCs to decrease the thermal conductivity as well as increase strain compliance. We provide an overview of recently identified low thermal conductivity oxides and discuss the mechanisms involved in the minimization of the thermal conductivity.

Yttria-stabilized zirconia

The most widely used TBC material is YSZ, zirconia containing 6–8 wt% Y_2O_3 (equivalent to about 3.4–4.5 mol%), which is produced in a metastable tetragonal phase (t').[2] Alloying zirconia with yttria is necessary to avoid the disruptive monoclinic to tetragonal phase transformation that would otherwise cause mechanical breakdown of the zirconia; however, it also reduces the thermal conductivity by creating point defects that scatter phonons. The introduction of Y^{3+} as an aliovalent dopant on the Zr^{4+} site is compensated by vacant oxygen sites. Interestingly, because of the similarity in atomic mass between the Y^{3+} and Zr^{4+} ions, the oxygen vacancies are primarily responsible for reducing thermal conductivity.

A physical picture of thermal transport in solids is given by propagating lattice waves, known as phonons. Scattering of these waves off of each other, as well as off of the defects in

Wei Pan, State Key Lab of New Ceramics and Fine Processing, Tsinghua University, Beijing, China; panw@mail.tsinghua.edu.cn
Simon R. Phillpot, Department of Materials Science and Engineering, University of Florida, Gainesville, FL; sphil@mse.ufl.edu
Chunlei Wan, Graduate School of Engineering, Nagoya University, Nagoya, Japan; chunlei.wan@gmail.com
Aleksandr Chernatynskiy, Department of Materials Science and Engineering, University of Florida, Gainesville, FL; avtche01@gmail.com
Zhixue Qu, College of Materials Science and Engineering, Beijing University of Technology, Beijing, China; quzhixue@bjut.edu.cn
DOI: 10.1557/mrs.2012.234

© 2012 Materials Research Society

https://doi.org/10.1557/mrs.2012.234 Published online by Cambridge University Press

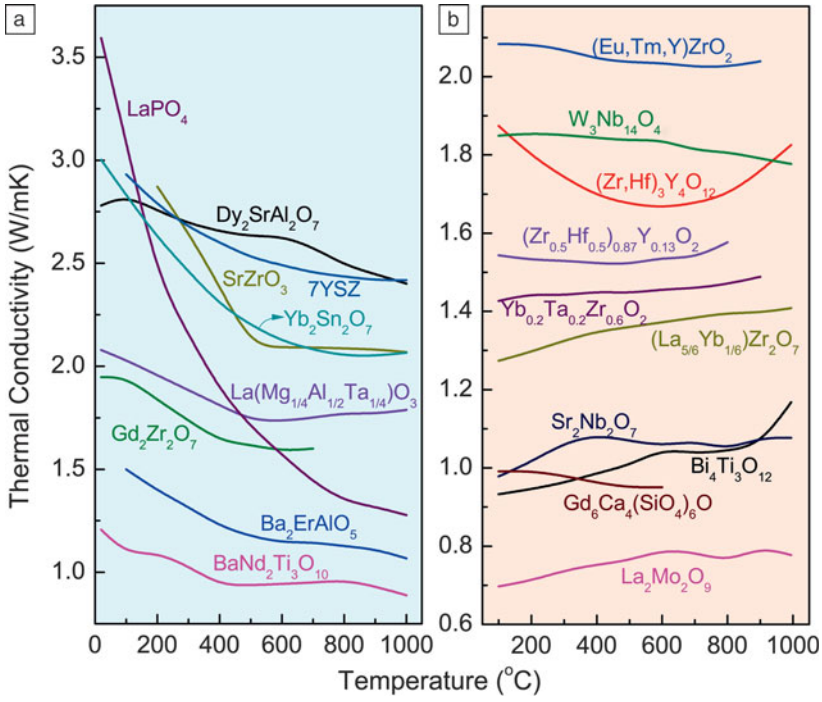


Figure 1. (a) Thermal conductivity summary of the emerging ceramics for thermal-barrier coatings, whose conductivities vary with temperature, including 7YSZ,[23] $Gd_2Zr_2O_7$,[22] $Yb_2Sn_2O_7$,[21] $SrZrO_3$,[29] $La(Mg_{1/4}Al_{1/2}Ta_{1/4})O_3$,[31] Ba_2ErAlO_5,[32] $Dy_2SrAl_2O_7$,[33] $BaNd_2Ti_3O_{10}$, and $LaPO_4$;[38] (b) temperature-independent thermal conductivities of ceramics, including $Yb_{0.2}Ta_{0.2}Zr_{0.6}O_2$,[13] $(La_{5/6}Yb_{1/6})Zr_2O_7$,[27] $Gd_6Ca_4(SiO_4)_6O$,[40] $La_2Mo_2O_9$,[23] $Bi_4Ti_3O_{12}$,[35] $(Zr,Hf)_3Y_4O_{12}$,[23] $(Eu,Tm,Y)ZrO_2$, $W_3Nb_{14}O_4$,[23] $Sr_2Nb_2O_7$, and $(Zr_{0.5}Hf_{0.5})_{0.87}Y_{0.13}O_2$.

the crystal lattice, impedes energy flow and pronounces itself as a thermal resistivity. Although models for the reduction in thermal conductivity from point defects based on this physical picture describe the basic mechanisms well,[3] molecular dynamics simulations reveal a more complex situation in YSZ. Interestingly, the physics is very similar in off-stoichiometric fluorite-structured UO_2, the dominant fuel system for nuclear fission reactors.[4,5] These studies show that with increasing defect concentration, the thermal conductivity transitions from that characteristic of a crystalline material to that characteristic of an amorphous solid.[6] This transition can be described in terms of the structure of the vibrational modes of the system. These can be classified as propagons (normal phonon modes that are delocalized with well-defined momentum and polarization), diffusons (delocalized like phonons, but no longer possessing well-defined polarizations), and locons (strongly localized modes). While the vibrational modes in a crystalline solid are essentially all propagons, the vibrations in amorphous materials contain diffusons (~93% of all modes in a-Si); these modes are far less efficient heat carriers. In both YSZ and UO_2, propagon modes only appear at the low-frequency end of the spectrum (<2 THz), while locons are concentrated at the high end (>26 THz). In the case of YSZ, complete transition to amorphous-like heat transport dominated by the diffusons takes place at about 24 YSZ (24% yttria): further increase of the Y_2O_3 content does not affect the structure of the vibrational spectrum. These molecular dynamics simulations indicate that more detailed exploration of the different forms of phonons in other complex oxides should be especially insightful.

The limitation in using YSZ at much higher temperatures than currently used is that the metastable tetragonal (t') phase partitions by diffusion into the equilibrium tetragonal (t) and cubic phases (c) at high temperatures; the former of which will transform into a monoclinic phase (m) during cooling, resulting in disintegration of the coating. This is a slow process, taking more than 100 hr at temperatures in excess of 1350°C before monoclinic zirconia is detectable.[7] To slow down this transformation and also lower the thermal conductivity, stabilizers other than yttria have been sought. Stabilization with rare-earth oxides, such as Gd_2O_3, Yb_2O_3, and Nd_2O_3, results in lower thermal conductivities than that of YSZ[8,9] as a result of larger mass difference between the dopant and zirconia. However, with the exception of Yb_2O_3, these ions actually decrease the resistance to destabilization of the t' phase.[10]

Co-doping zirconia with two or more oxides, one a trivalent oxide such as Y_2O_3 and the other a pentavalent oxide such as Nb_2O_5 or Ta_2O_5, has been shown to reduce the thermal conductivity.[11,12] Of particular interest is the compositional range over which the concentrations of trivalent and pentavalent ions are equal. In this range, a stable non-transformable tetragonal zirconia can form, with thermal conductivity almost half that of the conventional YSZ, despite the absence of oxygen vacancies.[11–13] Moreover, yttria can be replaced by other heavier rare-earth oxides, which can further reduce the thermal conductivity to 1.4 W m^{-1} K^{-1} at 900°C for Yb-Ta co-doped zirconia.[13,14]

A further route to optimizing the performance involves the addition of paired dopants, such as Nd_2O_3 (or Gd_2O_3) and Yb_2O_3 (and/or Sc_2O_3), into the ZrO_2-Y_2O_3 system, which segregate into 5–100 nm defect clusters and can reduce the thermal conductivity by about 20–40%, compared with the baseline ZrO_2-Y_2O_3 ceramics.[15–17] Meanwhile, these thermodynamically immobile defect clusters can significantly enhance the sintering resistance of the coating at high temperatures.

Pyrochlore materials

Increasing the complexity of the crystal structure tends to reduce the thermal conductivity due to the increasing number of optical phonons that tend not to contribute substantially to the thermal conductivity. This is primarily due to typically small group velocities of the optical phonons as compared to acoustic phonons. Additionally, increasing the number of optical states also increases the number of available phonon-phonon interactions, further reducing thermal conductivity.

https://doi.org/10.1557/mrs.2012.234 Published online by Cambridge University Press

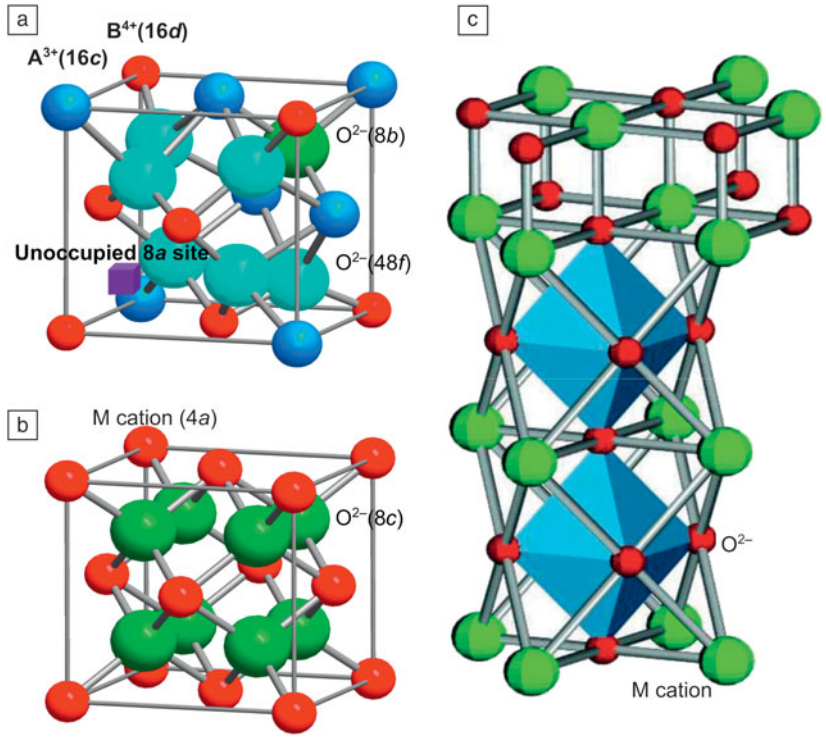


Figure 2. (a) A 1/8 unit cell of the $A_2B_2O_7$-type pyrochlore structure that can be adopted by low thermal conductivity rare-earth zirconates (A = rare earth element, B = Zr), indicating lattice sites and the unoccupied oxygen position. (b) The defect fluorite structure that can be induced in heavier rare-earth zirconates or by heat treatment of pyrochlore-type $Gd_2Zr_2O_7$ and shows similar thermal conductivities to the pyrochlores. In this structure, the cations are completely disordered, and the occupancy for each anion site is 0.875.[33] (c) An example of a perovskite-structured oxide: The layered Ruddlesden–Popper phase of Sr-Ti-O.[34] The oxygen octahedra of the two perovskite unit cells are outlined in blue, and the single rock salt layer is shown at the top.

The $A_2B_2O_7$-pyrochlore structure is one of a number of more complex crystal structures based on the fluorite structure of zirconia. It has a unit cell consisting of eight fluorite-like subcells, each of which contains one vacant oxygen site defect (the subcell of the pyrochlore structure is shown in **Figure 2a**). Both the presence of vacant sites and the larger unit cell should lower the thermal conductivity. Indeed, pyrochlore compounds of rare earth zirconates (where A= rare-earth element and B = Zr) exhibit extremely low thermal conductivity, ranging from ~1.1–1.7 W m^{-1} K^{-1} at temperatures between 700°C and 1200°C for A = La, Eu, Sm, Nd, and Gd.[18] The stability of the pyrochlore structure is sensitive to the ratio of the A and B cation radii.[19] Thermal conductivity simulations have been performed on the large family of pyrochlores with A = La, Pr, Nd, Sm, Eu, Gd, Y, Er, or Lu and B = Ti, Mo, Sn, Zr, or Pb.[20] **Figure 3** presents the resultant map of the thermal conductivity as a function of the A and B ionic radii. Of particular note is that increasing the B-cation radii consistently reduces thermal conductivity, whereas the A cation size has less of an effect. As yet, there is insufficient experimental data to confirm the details of this property map.[21] Large rare-earth ions in $Ln_2Zr_2O_7$ (Ln = La, Nd, Sm, Gd) can lead to a stable pyrochlore structure up to at least 1500°C.[22] $Gd_2Zr_2O_7$ can also take on a defected fluorite structure (Figure 2b) if suitably heat-treated, but the thermal conductivity was found to be the same as its pyrochlore counterpart.[22] It is interesting to note that a different defective fluorite structure, the delta-phase, is formed with smaller rare-earth ions, such as Dy, Er, Yb, and Y, and that these too have thermal conductivity similar to those of pyrochlores.[23,24]

The expectation that doping and alloying will reduce thermal conductivity is borne out experimentally. Some success has been achieved, at least up to ~800°C, as exemplified by $La_2Zr_2O_7$, which when doped with 30 at.% Gd displays a decrease in thermal conductivity from ~1.55 W m^{-1} K^{-1} to ~0.9 W m^{-1} K^{-1}.[25] In addition to lowering the thermal conductivity due to alloy scattering, doping can change the pyrochlore structure itself in ways that affect the thermal conductivity.[26] For example, in the $(Sm_{1-x}Yb_x)_2Zr_2O_7$ series, there is a transition from pyrochlore to a more disordered fluorite state when the x value lies between 1/6 and 1/3, at which there is also a dip in the thermal conductivity.[26] By contrast, in $(La_{1-x}Yb_x)_2Zr_2O_7$, the Yb^{3+} was found to "rattle" (undergo very large localized thermal vibration) at the 16 c-site, which could lead to a glass-like thermal conductivity.[27] Among the mentioned pyrochlores, some oxides such as $Sm_2Zr_2O_7$, $Gd_2Zr_2O_7$, and their composites may become the potential materials for TBCs, owing to the better comprehensive mechanical and thermal performances.

Perovskite-structured oxides

The ABO_3-type perovskites are another class of material that show both a large number of options for the A and B

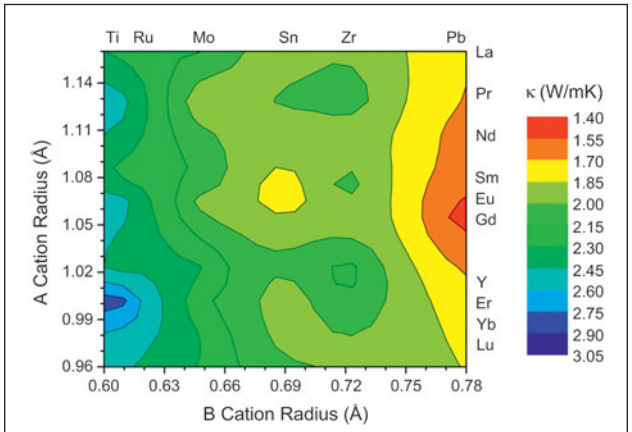


Figure 3. Contour map of thermal conductivity (κ) determined at T = 1473 K by simulation, as a function of ionic radii of the A and B ions for pyrochlore $A_2B_2O_7$.[20]

https://doi.org/10.1557/mrs.2012.234 Published online by Cambridge University Press

cations, and display a large number of structural variants.[28] They therefore seem to be good candidates for engineering the thermal conductivity. Pure ABO_3 perovskites containing high atomic mass ions exhibit low thermal conductivities, for example, 2.1 W m^{-1} K^{-1} for $SrZrO_3$[29] and 3.4 W m^{-1} K^{-1} for $BaZrO_3$[18] at 1000°C on account of the structural rigidity of corner-shared octahedra.[29] However, following the strategy that was so successful for fluorite, Yb_2O_3 has been doped onto the B site of $SrZrO_3$, leading to a 20% reduction in the thermal conductivity over the temperature range of 200–1200°C.[30] Moreover, increasing the doping level can lead to new complex perovskite structures. For example, $Ba(Mg_{1/3}Ta_{2/3})O_3$ has a melting temperature of ~3000°C and is considered among the most refractory of all oxides;[15] its thermal conductivity reaches 2.5 W m^{-1} K^{-1} at 1100°C. Likewise, the $La(Al_{1/4}Mg_{1/2}Ta_{1/4})O_3$ complex perovskite system shows a low value of thermal conductivity (~2 W m^{-1} K^{-1}) and high coefficient of thermal expansion (~11.9 × 10^{-6} K^{-1}), which is a promising combination for TBC applications. However, TBCs made of these complex perovskites show short thermal cycling life, possibly due to their low toughness and consequent weak thermal shock resistance.[31]

Bearing a similar relationship to the perovskite structure as the pyrochlore structure does to fluorite, Ba_2LnAlO_5 (Ln = lanthanide element), in which one-sixth of the oxygen sites in the perovskite structure are vacant, has a thermal conductivity of only 1.1 W m^{-1} K^{-1} at 1000°C.[32] Again following the strategy of increasing the size of the unit cell and increasing the number of atoms per unit cell, thereby increasing the number of optical phonons and reducing the thermal conductivity, the perovskite structure can also be a building block for complex superlattice structures. The thermal conductivities of Ruddlesden–Popper (RP) structures of $Ln_2SrAl_2O_7$[33] and $Sr_{n+1}Ti_nO_{3n+1}$[34] (**Figure 2**c), the Aurivillius phases[35] of $Bi_4Ti_3O_{12}$, and the Dion–Jacobson phases of $BaLa_2Ti_3O_{10}$[36] have been studied, all producing thermal conductivities of 1–2 W m^{-1} K^{-1}, which are substantially lower than the typical value of 2.5 W m^{-1} K^{-1} for 7YSZ. As shown in Figure 2c, the RP structure consists of n (n = 1, 2,...) layers of perovskite structured material separated by a rock salt structured layer; the Aurivillius and Dion–Jacobson phases show analogous layered perovskite structures.

Lanthanide orthophosphates and silicates

The lanthanide orthophosphates ($LnPO_4$) are another set of compounds with low thermal conductivities.[37] The orthophosphates can take on either a monazite or xenotime crystal structure, depending on the ionic size of the lanthanide ions. Monazite $LnPO_4$ (Ln = La-Gd) is expected to show a distinctly lower thermal conductivity than the xenotime structure compounds due to its lower crystal symmetry and weaker bonds.[23,38] The anisotropy of thermal conductivity of the most studied monazite compound $LaPO_4$ is also noticeable, due to the non-cubic crystal structure.[39] However, the characteristics of the line compound (small deviations from the stoichiometry can significantly change the solidus temperature, thereby making it hard to apply the plasma spraying process to make coatings) and poor adherence to the bond-coat layer (between the TBC and the superalloy) limits the applications of $LaPO_4$ as a TBC.[37]

Based on their large unit cell and complex structures, the rare-earth silicates (**Figure 4**) can be expected to yield low thermal conductivity values. Among these, apatite structured $Gd_8Ca_2(SiO_4)_6O_2$ has attracted particular attention;[40] it exhibits an extremely low and temperature-independent thermal conductivity of about 1.4 W m^{-1} K^{-1} for almost fully dense samples. Another interesting feature of this compound is that the composition can be systematically altered by adjusting the relative proportions of alkaline earth cations and rare-earth ions to introduce different populations of oxygen vacancies, cation vacancies, and oxygen interstitials, resulting in even lower thermal conductivities for defect-containing compositions (**Figure 5**).[40]

Thermal expansion coefficient

While thermal conductivity is the key performance metric for potential TBC materials, it is also essential that they be thermomechanically compatible with both the superalloy that they coat and the intermediate bonding layers (see the introductory article in this issue). The thermal expansion coefficient of YSZ is 10.7 × 10^{-6} K^{-1} from room temperature to 1273 K,[41] while those of the typical superalloy substrate and bond coat (NiCrAlY) are 16 × 10^{-6} K^{-1} and 17.5 × 10^{-6} K^{-1}, respectively, for the same temperature range.[41] This mismatch can lead to high thermal stresses that have the potential to promote coating failure. Although YSZ coatings can last tens of thousands of hours and multiple cycling without failing, it is still believed

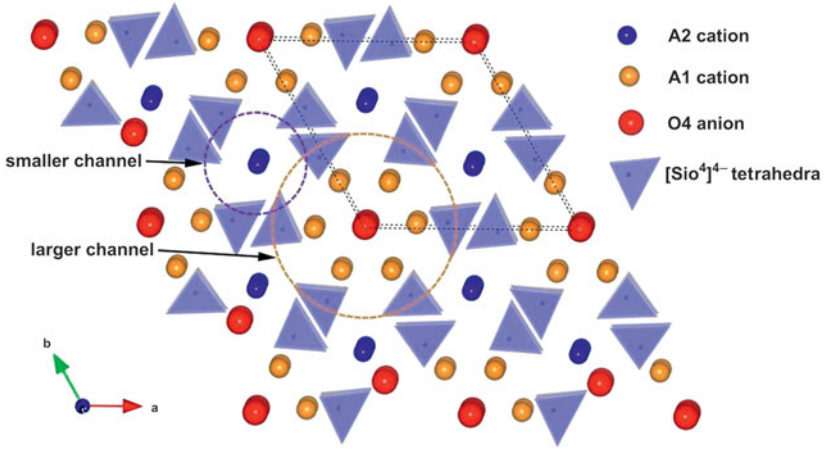


Figure 4. View of the crystal structure of the stoichiometric rare-earth apatites $A_{10}(SiO_4)_6O_{2+\delta}$, along the [001] axis, and the location of the two types of cation sites, A1 and A2, as well as the oxygen sites, O4.[40] The complexity and large unit cell of this structure is believed to give rise to low thermal conductivity in materials such as $Gd_8Ca_2(SiO_4)_6O_2$.

https://doi.org/10.1557/mrs.2012.234 Published online by Cambridge University Press

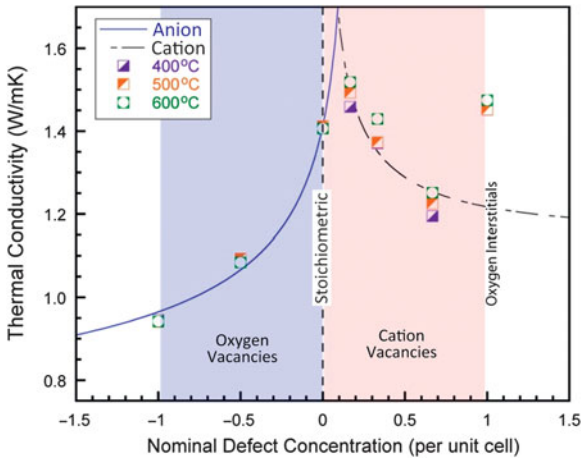


Figure 5. Thermal conductivity of rare-earth apatites in the range 400–600°C as a function of nominal defect concentration per unit cell. One defect per unit cell corresponds to a concentration of 2.5 at.%.[40] The thermal conductivities agree well with the trend predicted by the simple defect scattering model, in which the thermal conductivities are proportional to the inverse square root of the anion and cation vacancy concentrations.

that enhancement of the thermal expansion coefficients of TBCs could minimize this mismatch and thereby further improve the thermal cycling lifetime of TBCs. Ceria (CeO_2), which has a high thermal expansion coefficient and relatively low thermal conductivity, has been found to improve the thermal expansion behavior of zirconia-based ceramics. For example, Sodeoka et al.[42] observed that the average thermal expansion coefficient of pure zirconia over the range of 25–800°C increases to 12.5×10^{-6} K^{-1} with the addition of CeO_2. Moreover, Cao et al.[43] proposed lanthanum-cerium oxide ($La_2Ce_2O_7$) as a potential TBC material; it has a thermal expansion coefficient as high as about 13×10^{-6} K^{-1} at elevated temperature, though it displays a sharp decrease between 180°C and 300°C. The thermal expansion coefficient of pyrochlore-type $Sm_2Zr_2O_7$ can be improved from 10.8×10^{-6} K^{-1} [22] to 11.9×10^{-6} K^{-1} [44] with 7.5 mol% doping of MgO, as the relatively smaller Mg^{2+} can easily get into the interstitial site of the crystal, thereby weakening the bonds of ZrO_6 octahedra. These successes notwithstanding, there remains a substantial gap between the thermal expansion coefficients of TBC materials and the bond coat and alloy.

Conclusions and outlook

The fluorite system provides a blueprint for a successful design strategy of starting with a crystal structure that can accommodate a large number of different chemical species and making it chemically and structurally more complex, has proven fruitful in developing low thermal conductivity materials for possible thermal-barrier coating (TBC) applications. This strategy is now being used in the context of perovskite materials, particularly through layering. The rich complexities of other oxide crystal systems remain largely unexplored for TBC applications. To move beyond an Edisonian approach to these materials, a more detailed fundamental understanding of thermal transport mechanisms is still required. Moreover, to truly accelerate the development of new TBCs, an integrated strategy of design for thermal management, thermomechanical, and chemical stability is required. This remains a challenge for the TBC community.

Acknowledgments

The work described has been supported, in part, by several agencies. The work of W.P., C.W., and Z.Q. was supported by the National Natural Science Foundation of China (Grant No. 51072088, 50990302) as well as through the US National Science Foundation through a World Materials Network grant. SRP and AC are subcontractors of the US Government under DOE Contract No. DE-AC07–05ID14517, under the Energy Frontier Research Center (Office of Science, Office of Basic Energy Science, FWP 1356). The US Government retains a worldwide license to publish or reproduce the published form of this manuscript, or allow others to do so, for US Government purposes.

References

1. R. Siegel, C.M. Spuckler, *Mater. Sci. Eng., A* **245**, 150 (1998).
2. S. Stecura, "Optimization of the NiCrAl-Y/ZrO_2-Y_2O_3 Thermal Barrier System" (NASA Tech. memo, Cleveland, 1985).
3. J. Callaway, H.C. von Baeyer, *Phys. Rev.* **120** (4), 1149 (1960).
4. P.K. Schelling, S.R. Phillpot, *J. Am. Ceram. Soc.* **84** (12), 2997 (2001).
5. T. Watanabe, S.G. Srivilliputhur, P.K. Schelling, J.S. Tulenko, S.B. Sinnott, S.R. Phillpot, *J. Am. Ceram. Soc.* **92** (4), 850 (2009).
6. P.B. Allen, J.L. Feldman, S.R. Bickham, *Philos. Mag. B* **79** (11–12), 1715 (1999).
7. V. Lughi, D.R. Clarke, *Surf. Coat. Technol.* **200** (5–6), 1287 (2005).
8. J. Feng, X.R. Ren, X. Wang, R. Zhou, W. Pan, *Scripta Mater.* **66** (1), 41 (2012).
9. M.N. Rahaman, J.R. Gross, R.E. Dutton, H. Wang, *Acta Mater.* **54** (6), 1615 (2006).
10. C.G. Levi, *Curr. Opin. Solid State Mater. Sci.* **8** (1), 77 (2004).
11. S. Raghavan, H. Wang, R.B. Dinwiddie, W.D. Porter, R. Vaβen, D. Stöver, M.J. Mayo, *J. Am. Ceram. Soc.* **87** (3), 431 (2004).
12. S. Raghavan, H. Wang, W.D. Porter, R.B. Dinwiddie, M.J. Mayo, *Acta Mater.* **49** (1), 169 (2001).
13. Y. Shen, R.M. Leckie, C.G. Levi, D.R. Clarke, *Acta Mater.* **58** (13), 4424 (2010).
14. X.W. Song, M. Xie, R. Mu, F. Zhou, G. Jia, S. An, *Acta Mater.* **59** (10), 3895 (2011).
15. M.O. Jarligo, D.E. Mack, G. Mauer, R. Vaβen, D. Stöver, *J. Therm. Spray Technol.* **19** (1–2), 303 (2010).
16. R. Vaβen, M.O. Jarligo, T. Steinke, D.E. Mack, D. Stöver, *Surf. Coat. Technol.* **205** (4), 938 (2010).
17. D.M. Zhu, R.A. Miller, *Int. J. Appl. Ceram. Technol.* **1** (1), 86 (2004).
18. R. Vaβen, X.Q. Cao, F. Tietz, D. Basu, D. Stöver, *J. Am. Ceram. Soc.* **83** (8), 2023 (2000).
19. B.J. Wuensch, K.W. Eberman, *J. Miner.* **52**, 19 (2000).
20. P.K. Schelling, S.R. Phillpot, R.W. Grimes, *Philos. Mag. Lett.* **84** (2), 127 (2004).
21. Z. Qu, C. Wan, W. Pan, *Acta Mater.* **60** (6–7), 2939 (2012).
22. J. Wu, X.Z. Wei, N.P. Padture, P.G. Klemens, M. Gell, E. Garcia, P. Miranzo, M.I. Osendi, *J. Am. Ceram. Soc.* **85** (12), 3031 (2002).
23. M.R. Winter, D.R. Clarke, *J. Am. Ceram. Soc.* **90** (2), 533 (2007).
24. Q. Xu, W. Pan, J. Wang, C. Wan, L. Qi, H. Miao, K. Mori, T. Torigoe, *J. Am. Ceram. Soc.* **89** (1), 340 (2006).
25. H. Lehmann, D. Pitzer, G. Pracht, R. Vaβen, D. Stöver, *J. Am. Ceram. Soc.* **86** (8), 1338 (2003).
26. C.L. Wan, Z.X. Qu, A. Du, W. Pan, *J. Am. Ceram. Soc.* **94** (2), 592 (2011).
27. C.L. Wan, W. Zhang, Y. Wang, Z.X. Qu, A. Du, R. Wu, W. Pan, *Acta Mater.* **58** (18), 6166 (2010).
28. R.H. Mitchell, *Perovskites: Modern and Ancient* (Almaz Press, Thunder Bay, 2002).
29. W. Ma, D.E. Mack, R. Vaβen, D. Stöver, *J. Am. Ceram. Soc.* **91** (8), 2630 (2008).
30. W. Ma, M.O. Jarligo, D. Pitzer, J. Malzbender, R. Vaβen, D. Stöver, *J. Therm. Spray Technol.* **17** (5–6), 831 (2008).

https://doi.org/10.1557/mrs.2012.234 Published online by Cambridge University Press

31. M.O. Jarligo, D.E. Mack, R. Vaβen, D. Stöver, *J. Therm. Spray Technol.* **18** (2), 187 (2009).
32. C. Wan, Z. Qu, Y. He, D. Luan, W. Pan, *Phys. Rev. Lett.* **101** (8), 085901 (2008).
33. C.L. Wan, T.D. Sparks, W. Pan, D.R. Clarke, R. David, *J. Am. Ceram. Soc.* **93** (5), 1457 (2010).
34. A. Chernatynskiy, R.W. Grimes, M.A. Zurbuchen, D.R. Clarke, S.R. Phillpot, *Appl. Phys. Lett.* **95** (16) (2009).
35. Y. Shen, D.R. Clarke, P.A. Fuierer, *Appl. Phys. Lett.* **93** (10) (2008).
36. H. Guo, H. Zhang, G. Ma, S. Gong, *Surf. Coat. Technol.* **204** (5), 691 (2009).
37. X.Q. Cao, R. Vaβen, D. Stöver, *J. Eur. Ceram. Soc.* **24** (1), 1 (2004).
38. A.B. Du, C.L. Wan, Z. Qu, W. Pan, *J. Am. Ceram. Soc.* **92** (11), 2687 (2009).
39. A.B. Du, C.L. Wan, Z. Qu, R. Wu, W. Pan, *J. Am. Ceram. Soc.* **93** (9), 2822 (2010).
40. Z.X. Qu, T.D. Sparks, W. Pan, D.R. Clarke, *Acta Mater.* **59** (10), 3841 (2011).
41. R. Vaβen, G. Kerkhof, D. Stöver, *Mater. Sci. Eng., A* **303** (1–2), 100 (2001).
42. S. Sodeoka, M. Suzuki, K. Ueno. H. Sakuramoto, T. Shibata, M. Ando, *J. Therm. Spray Technol.* **6** (3), 361 (1997).
43. X.Q. Cao, R. Vaβen, W. Fischer, F. Tietz, W. Jungen, D. Stöve, *Adv. Mater.* **15** (17), 1438 (2003).
44. Z.X. Qu, C.L. Wan, W. Pan, *Chem. Mater.* **19** (20), 4913 (2007). □

CAREER CENTER

2012 MRS FALL MEETING

Meet Your Next Employer …

Show off your talents to the world's most prestigious universities, laboratories and high-tech firms. FREE of charge to all MRS Members, the Career Center provides targeted employment opportunities to candidates seeking positions in the scientific community.

- Review open positions tailored to the materials research industry
- Interview with prospective employers
- Visit on-site recruitment booths and network with technical staff

For additional information, visit **www.mrs.org/fall2012**

Hynes Convention Center
Level 2, Hall C

Registration:
Monday, November 26
1:00 pm – 4:00 pm

Hours:
Tuesday, November 27
11:00 am – 5:00 pm
Wednesday, November 28
11:00 am – 5:00 pm
Thursday, November 29
10:00 am – 1:30 pm

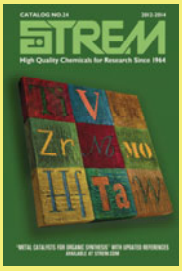
Do the research to advance your career…visit the MRS Career Center in Boston!

STREM Chemicals, Inc.
An Employee-Owned Company Serving Customers Globally

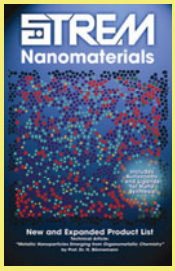
Established 1964

Visit www.strem.com/mrs for more information.

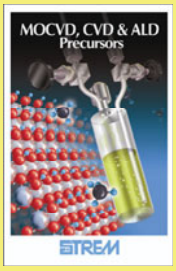
Catalog of Chemicals for R&D



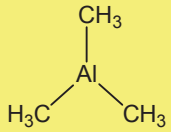
Nano Products



CVD/ALD Precursors



- Chemicals for R&D
- Nanomaterials
- High Purity Inorganics
- CVD/ALD Precursors
- Bubblers & Cylinders



93-1360



97-3425

PURE NP's via laser ablation



Quantum Dots



Bubblers/Cylinders



Corporate Headquarters
Newburyport, MA 01950 USA · email: info@strem.com

Europe
67800 Bischheim, France · email: info.europe@strem.com

website: www.strem.com

https://doi.org/10.1557/mrs.2012.234 Published online by Cambridge University Press